

Modulated structures in tilted chiral smectic films

A. E. Jacobs

Department of Physics and Scarborough College, University of Toronto, Toronto, Ontario, Canada M5S 1A7

Galya Goldner

Department of Chemical Physics, The Weizmann Institute of Science, Rehovot, Israel

David Mukamel

Department of Physics, The Weizmann Institute of Science, Rehovot, Israel

(Received 17 September 1991)

The structure of the modulated phases that can occur in systems like chiral tilted smectic films and monolayers of tilted amphiphiles is studied numerically within the mean-field approximation. Two types of modulated phases, uniaxial and hexagonal, are considered. The uniaxial phase is composed of an array of nontopological line defects and is therefore different from modulated structures occurring near ordinary commensurate-incommensurate phase transitions. The hexagonal phase displays point defects and topological π line defects. We discuss the energetics of these structures and the nature of the modulated-smectic-*C* phase transition.

PACS number(s): 64.70.Md, 61.30.Jf, 61.30.Gd, 68.10.-m

I. INTRODUCTION

Freely suspended thin films of tilted smectic liquid crystals have been studied extensively in recent years [1-6]. This system provides an easily accessible realization of two-dimensional *XY*-type models. The free films are prepared by drawing liquid-crystal material across an opening in a thin flat support. Stable films as thin as two molecular layers can be obtained in this way, with the smectic layers parallel to the surface of the resulting film. In a series of experiments, two-dimensional melting, the existence of a hexatic phase [3], and bond-orientational order in the smectic-*I* phase [4] have been studied in these systems.

When the liquid crystal is composed of a nonracemic mixture of chiral molecules, a tilted smectic phase becomes ferroelectric [7], with polarization vector \mathbf{P} oriented parallel to the smectic layers and perpendicular to the local director \mathbf{n} . In describing the various structures and phase transitions in these systems, one may use the polarization $\mathbf{P} = (P_x, P_y)$ as an order parameter; we assume the smectic layers to be parallel to the *x-y* plane. It has been argued [8-15] that modulated structures may be induced by a $P^2 \nabla \cdot \mathbf{P}$ term which exists in the Landau-Ginzburg (LG) model associated with this system. Experimental indications for the existence of such structures have recently been reported [6].

We study these modulated structures in the mean-field approximation, using the following LG model corresponding to a chiral smectic-*C* layer:

$$H = \int d^2r \mathcal{H}[\mathbf{P}], \tag{1}$$

where the free-energy density is [16]

$$\mathcal{H} = a(1 - \Delta)(\nabla \cdot \mathbf{P})^2 + a(1 + \Delta)(\nabla \times \mathbf{P})^2 + \alpha P^2 - \beta P^2 \nabla \cdot \mathbf{P} + \gamma P^4. \tag{2}$$

As usual we assume that only the Landau coefficient α depends on temperature T . Some aspects of the phase diagram associated with this model have been studied previously. As shown in Fig. 1, the model exhibits a smectic-*A* (Sm-*A*) phase with $\mathbf{P}=0$, a smectic-*C* (Sm-*C*) phase with uniform \mathbf{P} , and modulated phases in which \mathbf{P} varies with position, forming a periodic structure. The LG model of (1) and (2) also describes phase transitions in monolayers of tilted amphiphiles at the air-water interface [17-19] and (with $\Delta = 0$) in certain ferroelectric crystals.

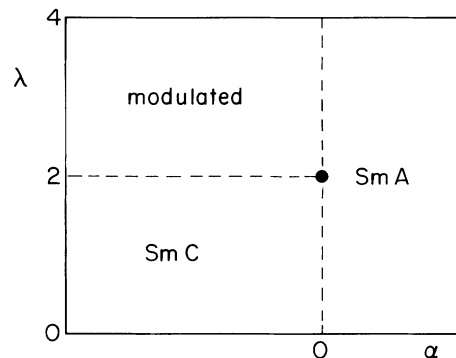


FIG. 1. Phase diagram in the α - λ plane for the model of Eqs. (1) and (2) with $\Delta = 0$; here $\lambda = \beta/\sqrt{\gamma a}$. The smectic-*A* (Sm-*A*), smectic-*C* (Sm-*C*), and modulated phases are stable in the regions indicated; all transitions are second order. The model is unstable for $\lambda \geq 4$ (see Ref. [15]). The modulated state in the figure is the uniaxial state. For large $\Delta > 0$, the hexagonal state described in Sec. III is the favored modulated state in part of the phase diagram, but details of the uniaxial-hexagonal and modulated-commensurate transitions have not been worked out in this case.

The transition from the smectic-*A* phase to the modulated structure has been studied in detail [8–10,15]. It has been argued [10,15] that this is a special kind of second-order transition, of neither instability nor nucleation type. The modulated structure in the model (1)-(2) is induced (driven) by the $P^2 \nabla \cdot \mathbf{P}$ term which is cubic in the order parameter. In contrast, the modulated structure in typical instability transitions is induced by a quadratic term, either a Lifshitz invariant of the form $(P_x \partial P_y / \partial z - P_y \partial P_x / \partial z)$ or a term such as $-(\nabla \eta)^2$ (for a system with a one-component order parameter). The order parameter vanishes as $(T_c - T)^{1/2}$ in all three cases, but the different form of the driving term gives the Sm-*A*-modulated transition and the modulated phase several features quite different from those in typical instability transitions. (1) The wave number q vanishes at the transition. (2) The harmonic content of the modulated structure is nontrivial even close to the transition point T_c ; explicitly, the ratios $P(n\mathbf{q})/P(\mathbf{q})$, $n > 1$, of the amplitudes of the higher harmonics to that of the fundamental remain finite at the transition. (3) The modulated structure near T_c is universal, and in particular it does not depend on the higher-order terms in the LG model (though these terms, such as δP^6 , change the structure at low temperatures).

To reduce the number of parameters, and to demonstrate the universal character, we scale the variables for the polarization and the position as $\mathbf{P} = \sqrt{-\alpha/\gamma} \boldsymbol{\sigma}$ and $\mathbf{r} = \sqrt{-a/\alpha} \mathbf{x}$; the scaled energy density $\bar{\mathcal{H}} = \mathcal{H}\gamma/\alpha^2$ is

$$\bar{\mathcal{H}} = (1 - \Delta)(\nabla \cdot \boldsymbol{\sigma})^2 + (1 + \Delta)(\nabla \times \boldsymbol{\sigma})^2 - \sigma^2 - \lambda \sigma^2 \nabla \cdot \boldsymbol{\sigma} + \sigma^4, \quad (3)$$

where $\lambda = \beta/\sqrt{\gamma a}$. The Euler-Lagrange equation in the ordered phase is

$$(1 - \Delta)\nabla(\nabla \cdot \boldsymbol{\sigma}) - (1 + \Delta)\nabla \times (\nabla \times \boldsymbol{\sigma}) + \boldsymbol{\sigma} - \lambda[\nabla(\sigma^2/2) - \boldsymbol{\sigma}(\nabla \cdot \boldsymbol{\sigma})] - 2\sigma^2 \boldsymbol{\sigma} = \mathbf{0}. \quad (4)$$

Note that the scaled density is independent of temperature, and hence the modulated structure is universal, depending on the two parameters λ and Δ .

The structure of the modulated phase has been considered previously. It has been suggested [9,12–14] that this phase is either uniaxial or hexagonal depending on the parameter Δ . The uniaxial structure corresponding to the model (1)-(2) with $\Delta = 0$ has been studied numerically in detail [15] and shown to be unlike other incommensurate structures. Furthermore, some general considerations concerning the nature of the modulated phase in the vicinity of the transition to the smectic-*C* (commensurate) phase have been presented [12–14]. In these analyses it was assumed that the modulated structure is obtained by condensation of walls which have negative energy, as in ordinary commensurate-incommensurate (CI) transitions. Several structures have been suggested, but the precise nature of the defects (e.g., whether they are topological objects) has not been explicitly demonstrated for the model (1)-(2); on the other hand, our previous numerical studies [15] demonstrated that the defects are non-topological in the uniaxial phase.

In the present paper, the modulated structures asso-

ciated with the Hamiltonian (1)-(2) are studied numerically within the mean-field approximation. We also consider in some detail the nature of the transition from the modulated phases to the commensurate (Sm-*C*) phase, and study the scaling properties of the modulated structure near the transition. Our main result is that in the vicinity of the transition to the smectic-*C* phase, the uniaxial phase is composed of an array of nontopological line defects, while the hexagonal phase displays point defects and topological π line defects. The energetics of these structures is also discussed. Section II describes the uniaxial phase and the transition to the commensurate phase, while Sec. III provides a similar analysis for the hexagonal phase. These are idealized structures, as we neglect macroscopic energy considerations, boundary effects, and the effects of charged impurities; we neglect also fluctuations (which are especially important for the uniaxial phase, as discussed at the end of Sec. II).

II. UNIAXIAL STRUCTURE

The density of Eq. (3) is rotationally and translationally invariant in the x - y plane. We consider uniaxial solutions modulated in the y direction, with σ_x and σ_y functions of y alone. Structures of period $L = 2\pi/q$ were obtained by solving the Euler-Lagrange equations (4); the corresponding free energy was calculated and optimized with respect to the wave number q . Figure 2 shows the amplitude and the phase of the uniaxial structure for several values of λ , at $\Delta = 0$, and Fig. 3 shows the vector field at $\lambda = 3$. These structures are ferroelectric, and macroscopic energy considerations and boundary conditions [12] may require domain walls.

In the following, we study the structure near the commensurate-incommensurate transition, which takes place at $\lambda = 2$, in more detail. As can be seen from Fig. 2, as $\lambda \rightarrow 2$ the amplitude of the order parameter takes on its commensurate value σ_c except in a narrow region (the core), in which the amplitude drops well below σ_c ; in the same limit, the phase changes rapidly in the core, reaching values $\pm\phi_0$, and then exhibits much slower (algebraic) variation outside the core. Some aspects of this behavior are similar to incommensurate structures near conventional second-order CI transitions (which are usually nucleation transitions). But there are major differences. (i) In ordinary CI transitions the defects are topological, but here they are nontopological (since the phase ϕ has the same asymptotic value on both sides of the core); therefore the structure can unwind and deform continuously to restore the commensurate state. (ii) The wave number q vanishes as the CI transition at $\lambda = 2$ is approached, not as the typical $1/\ln(\lambda - 2)$ but rather linearly, as $\lambda - 2$. (iii) Even near the CI transition, there are no regions where the order parameter is nearly commensurate: the approach of the phase to its limiting value is algebraic rather than exponential as in a typical incommensurate system.

The algebraic behavior of the phase is understood analytically as follows. We expand about the commensurate state as

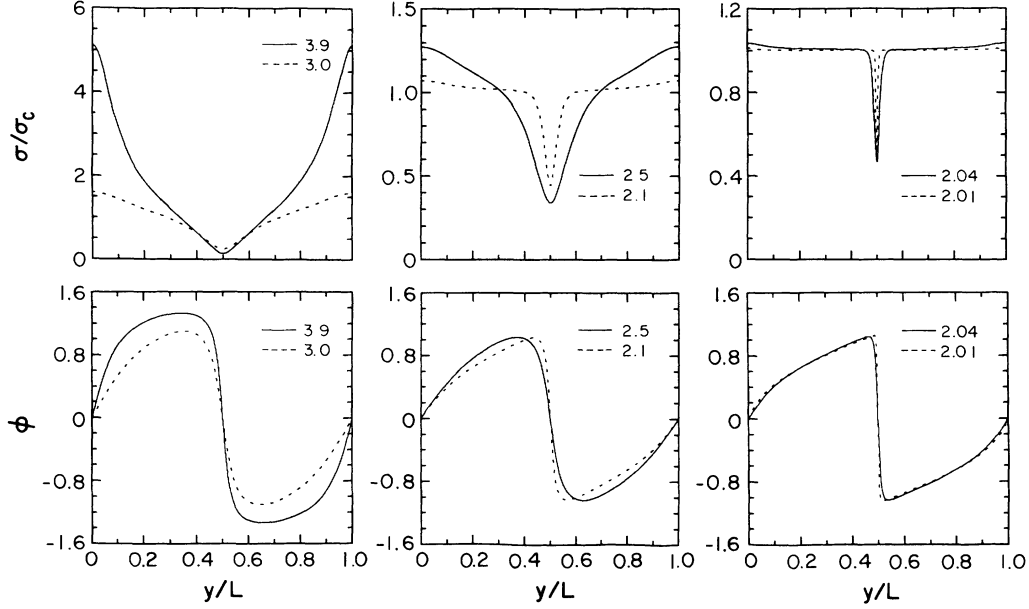


FIG. 2. Amplitude σ (relative to the commensurate value $\sigma_c = 1/\sqrt{2}$) and phase ϕ of the universal uniaxial structure as functions of the scaled position variable y/L (where $L = 2\pi/q$) for six values of the parameter λ ; the parameter Δ is zero. The plots are given for the optimal values of the wave number q (1.6653, 0.7642, 0.4846, 0.1437, 0.0642, and 0.0175 for $\lambda = 3.9, 3.0, 2.5, 2.1, 2.04,$ and 2.01 , respectively). Note that different scales are used in the frames for the amplitudes.

$$\sigma_x(y) = \sigma_c + \delta_x(y), \quad (5)$$

$$\sigma_y(y) = \delta_y(y);$$

the linearized Euler-Lagrange equations (for $\Delta = 0$) are

$$\delta_x'' + (\lambda/\sqrt{2})\delta_y' - 2\delta_x = 0, \quad (6)$$

$$\delta_y'' - (\lambda/\sqrt{2})\delta_x' = 0.$$

The solution for δ_x has the form

$$\delta_x = \begin{cases} \mathcal{S} + \text{const} & \text{for } \lambda > 2 \\ c_0 + c_1 y + c_2 y^2 & \text{for } \lambda = 2 \\ \mathcal{E} + \text{const} & \text{for } \lambda < 2 \end{cases} \quad (7)$$

where \mathcal{S} and \mathcal{E} represent sinusoidal and exponential terms, respectively. A combination of this result with the obvious solution for δ_y gives the algebraic behavior of the phase. The above analysis shows also that perturbations to the commensurate state decay exponentially only for $\lambda < 2$, and so the commensurate state is unstable for $\lambda > 2$. Generalizing to $\Delta \neq 0$, we find that the commensurate state is unstable for $\lambda > 2\sqrt{1-\Delta}$. The same stability limit is obtained when one considers more general nonuniaxial perturbations, where δ_x and δ_y are arbitrary functions of both x and y .

Obviously the conventional description of the incommensurate state as negative-energy defects repelling exponentially is entirely inappropriate for the uniaxial phase. But since this description is so appealing, it is natural to seek the counterpart for the uniaxial phase by examining the details of the energetics. Of course

the interpretation of the terms in the total free energy is not unique, because different representations of the free-energy density are possible; the model (1)-(2) is no different from conventional models in this respect. For example, if we modify the density of Eq. (3) by making the replacement

$$\lambda\sigma^2(\nabla \cdot \sigma) \rightarrow \lambda(\sigma^2 - \sigma_c^2)(\nabla \cdot \sigma), \quad (8)$$

then the differential equations and the total free energy are unchanged; more generally, because of the periodicity we can add to the density the divergence of any function

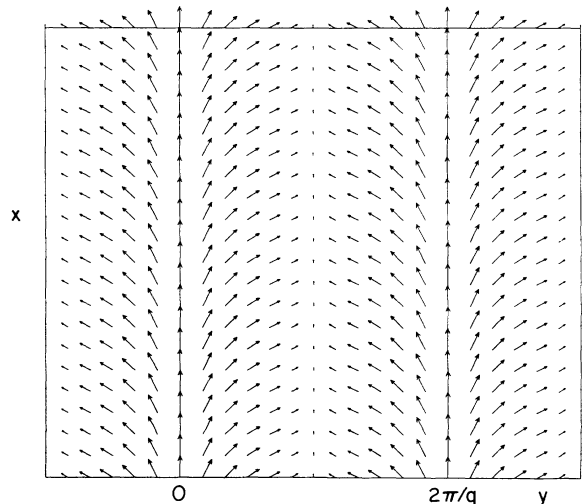


FIG. 3. Polarization of the uniaxial structure at $\lambda = 3$ and $\Delta = 0$; the wave number is optimal ($q = 0.7642$).

of σ_x and σ_y . If the free-energy density of Eq. (3) is used, the core energy (defined as the integral of the density over the core region) is positive rather than negative; the negative contribution to the total energy is a bulk term which comes from the slow variation of the phase outside the core. On the other hand, with the replacement of Eq. (8), the core energy is negative. This said, the density of Eq. (3) seems nonetheless the natural one, and we use it to construct a qualitative expression for the total energy (which is independent of the interpretation placed on the terms).

Using the representation of Eq. (3), we find the following expression for the energy per unit length E/L (here E is the energy of the structure relative to the energy of the commensurate phase, and $L = 2\pi/q$ is the period):

$$\frac{E}{L} = \frac{(a - b\lambda)}{L} + \frac{c}{L^2}, \quad (9)$$

where the parameters a , b , and c are positive. The core contributes the positive energy a ; the negative contribution $-b\lambda$ comes from the integral of $-\lambda\sigma^2\nabla\cdot\sigma$ outside the core; finally, the energy c/L is the elastic energy, corresponding to the variation of the phase ϕ outside the core. Note the difference in the interpretation as compared to the analysis of conventional incommensurate structures: here the negative energy comes from the bulk, rather than the core, while the positive energy comes from the core, rather than the bulk. We assume that the width of the core and the phase change ϕ_0 are independent of λ as the CI transition is approached; this implies that the parameters a , b , and c are also independent of λ in this limit, and therefore the CI transition can be analyzed using Eq. (9) with fixed a , b , and c . A form similar to Eq. (9) was suggested previously [13,14].

Minimizing the energy per unit length with respect to L , we find that the CI transition takes place when $(a - b\lambda) = 0$; stability analysis [see Ref. [9] and Eq. (7)] suggests that the transition occurs at $\lambda = 2$. Therefore our analysis predicts that L diverges as $1/(\lambda - 2)$, and that the energy per unit length vanishes as $(\lambda - 2)^2$, in agreement with our numerical results. Figure 4 shows that indeed the width of the core and the phase change ϕ_0 are independent of λ (in the limit $\lambda \rightarrow 2$), supporting the assumptions made in obtaining Eq. (9).

Since this system may show a hexagonal structure, we analyzed the linear stability of these uniaxial solutions to the nonuniaxial perturbations

$$\begin{aligned} \delta\sigma_x &= e^{ipx} s_x(y), \\ \delta\sigma_y &= e^{ipx} s_y(y); \end{aligned} \quad (10)$$

these are the forms appropriate for a system translationally invariant in the x direction. Uniaxial solutions of the differential equations were obtained for a wide range of λ and Δ values, including regions where the hexagonal phase is energetically favored. The eigenvalues of the Hessian matrix were calculated for arbitrary p and found to be all positive (apart from those corresponding to translations and rotations). Hence the uniaxial solutions are locally stable in all cases. As a further check on

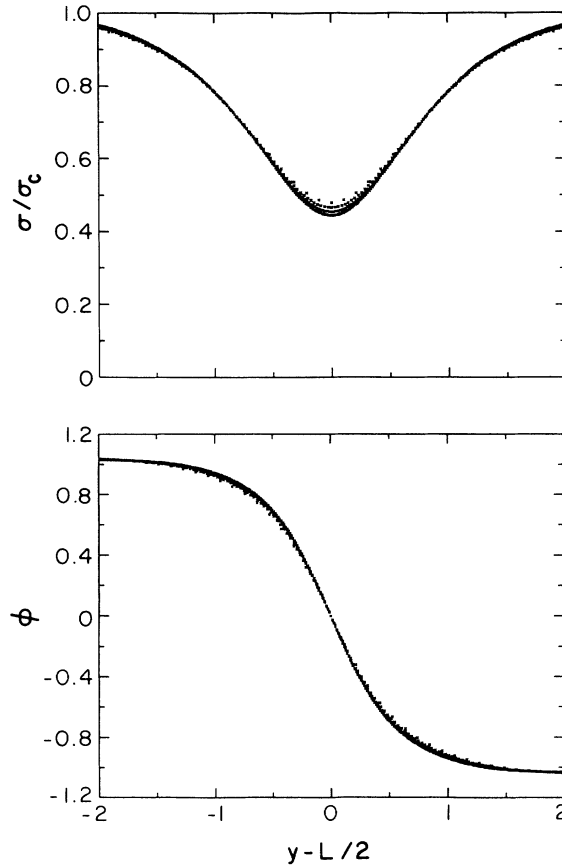


FIG. 4. Amplitude σ (relative to the commensurate value σ_c) and phase ϕ in the core of the uniaxial structure, plotted as functions of the unscaled distance from the center of the core, for $\lambda = 2.10, 2.07, 2.04$, and 2.01 , and $\Delta = 0$. It is evident that the width of the core and also the maximum phase ϕ_0 are independent of λ in the limit $\lambda \rightarrow 2$.

the stability of the uniaxial solutions, we verified that π domain walls have positive energy.

We conclude this section by commenting on the effect of thermal fluctuations on the uniaxial structure. It has been shown [20] that at finite temperatures, when both phonon and dislocation excitations are present, the correlations of the translational order parameter decay exponentially with distance in $d = 2$ dimensions. Although the uniaxial phase is unstable, and the Bragg peaks associated with this phase will be replaced by Lorentzian shapes, vestiges of the uniaxial phase may be observable; the correlation length can be large, and it may not be easy experimentally to distinguish true long-range order from short-range order.

III. HEXAGONAL STRUCTURE

This section considers solutions with hexagonal symmetry [12–14]. Since the hexagonal structure is predominantly radial, with small curl, while the uniaxial structure has large curl, one expects from Eq. (2) that the

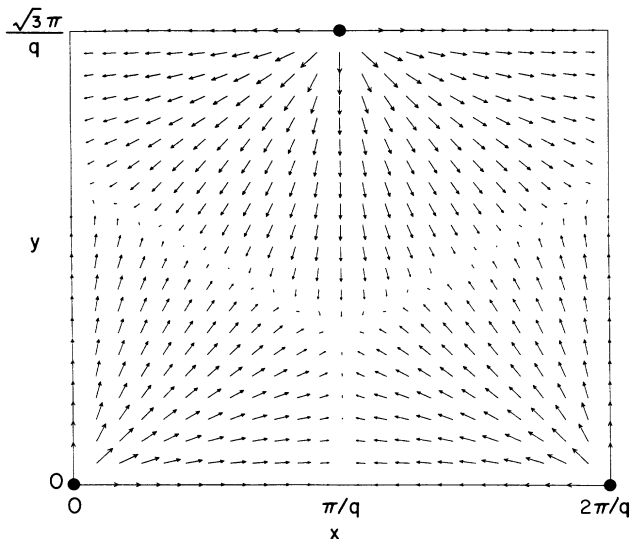


FIG. 5. Polarization of the hexagonal structure at $\lambda = 2.4$ and $\Delta = \frac{1}{3}$; the wave number is optimal ($q = 0.349$). The filled circles denote the forced nodes of the order parameter; other nodes occur at symmetry points like $(\pi/q, 0)$ and $(0, 2\pi/\sqrt{3}q)$.

hexagonal structure is favored at sufficiently large Δ [13, 14]. We have observed numerically the uniaxial to hexagonal transition (which is obviously first-order [13, 14]) with increasing Δ , but have not constructed the phase diagram in the λ - Δ plane. Figure 5 shows a typical hexagonal structure [21] (at parameter values where it has lower energy than the uniaxial phase), and Fig. 6 plots the order parameter along two symmetry directions. The main feature of the structure (which is topologically identical to that proposed previously [12–14]) is that the order parameter σ is predominantly radial. The order parameter vanishes at the center of the hexagon and at symmetry points on the boundary of the hexagonal cell; it is tangential on the boundaries, where its magnitude is markedly reduced. These boundaries are π line defects; apart from the different topology, they correspond to the core of the uniaxial phase.

We discuss next the energetics of the hexagonal structure for $\lambda \rightarrow 2$; in this limit, we expect the unit cell to increase in area. We also expect the order parameter to be radial in the bulk of the cell (with magnitude close to the commensurate value), and to be small along the boundary of the cell. Our numerical results are consistent with these assumptions, but have not been obtained close to the transition. From Eq. (3), such a structure gives the following energy per unit area:

$$\frac{E}{R^2} = \frac{(a' - b'\lambda)}{R} + \frac{c' \ln R}{R^2}, \quad (11)$$

where a' , b' , and c' are positive. The a' term gives the

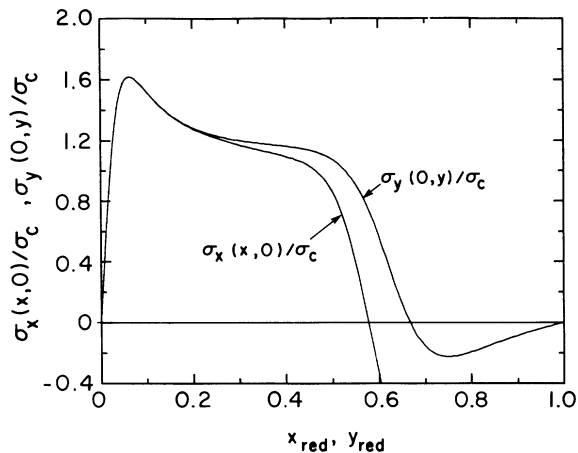


FIG. 6. $\sigma_x(x, 0)$ and $\sigma_y(0, y)$, the x and y components of the polarization σ in the hexagonal phase, along the x and y axes respectively; the polarization is radial (along the axis) in both cases. x_{red} and y_{red} are reduced coordinates defined by $(x_{\text{red}}, y_{\text{red}}) = q(x, y)/\sqrt{3}\pi$; the boundary of the Wigner-Seitz cell crosses the x axis at $x_{\text{red}} = 1/\sqrt{3}$, and the y axis at $y_{\text{red}} = \frac{2}{3}$. The parameters are the same as in Fig. 5 (which gives the full vector field).

contribution from the boundary of the hexagonal cell; the b' term comes from the integral of $-\lambda\sigma^2\nabla \cdot \sigma$ over the bulk of the cell, and the c' term comes from the elastic energy. The contribution of the region near $r = 0$ is negligible. A form similar to Eq. (11) has been suggested previously [13,14].

We discuss finally the possibility of a direct transition from the commensurate state to the hexagonal state. It is clear that if both terms $(a - b\lambda)$ and $(a' - b'\lambda)$ vanish at the same value of λ then the transition from the commensurate state is to the uniaxial state (since the elastic term is much larger for the hexagonal state), as discussed in Sec. II, and in Refs. [13] and [14]. It is not clear, however, that both terms vanish simultaneously: the defects in the two cases have different character; they are topological π line defects in the hexagonal case, but have no topological nature in the uniaxial case. There is no obvious reason that the two terms must vanish at the same point, and in principle a direct commensurate to hexagonal transition is possible if $(a' - b'\lambda)$ vanishes at a λ smaller than does $(a - b\lambda)$.

ACKNOWLEDGMENTS

This research was supported by the Natural Sciences and Engineering Research Council of Canada and by the US-Israel Binational Science Foundation, Jerusalem, Israel. G. Goldner acknowledges support from the Stone Foundation. We are grateful to J. Toner for comments on the manuscript.

- [1] D. E. Moncton and R. Pindak, *Phys. Rev. Lett.* **43**, 701 (1979).
- [2] J. Collett, P. S. Pershan, E. B. Sirota, and L. B. Sorensen, *Phys. Rev. Lett.* **52**, 356 (1984).
- [3] D. E. Moncton, R. Pindak, S. C. Davey, and G. S. Brown, *Phys. Rev. Lett.* **49**, 1865 (1982).
- [4] S. B. Dierker, R. Pindak, and R. B. Meyer, *Phys. Rev. Lett.* **56**, 1819 (1986); J. D. Brock, A. Aharony, R. J. Birgeneau, K. W. Evans-Lutterdot, J. D. Litster, P. M. Horn, G. B. Stephenson, and A. R. Tajbakhsh, *ibid.* **57**, 98 (1986).
- [5] D. H. Van Winkle and N. A. Clark, *Phys. Rev. A* **38**, 1573 (1988).
- [6] J. MacLennan, *Europhys. Lett.* **13**, 435 (1990).
- [7] R. B. Meyer, L. Liebert, L. Strzelecki, and P. Keller, *J. Phys. (Paris) Lett.* **36**, L-69 (1975).
- [8] S. Alexander, R. M. Hornreich, and S. Shtrikman, in *Symmetries and Broken Symmetries in Condensed Matter Physics*, edited by N. Boccara (Institut pour le Développement de la Science, l'Education et la Technologie, Paris, 1981), p. 379; A. L. Korzenevskii, *Zh. Eksp. Teor. Fiz.* **81**, 1071 (1981) [*Sov. Phys.—JETP* **54**, 568 (1981)].
- [9] D. Blankshtein, E. Domany, and R. M. Hornreich, *Phys. Rev. Lett.* **49**, 1716 (1982); D. Blankshtein and R. M. Hornreich, *Phys. Rev. B* **32**, 3214 (1985).
- [10] J. W. Felix, D. Mukamel, and R. M. Hornreich, *Phys. Rev. Lett.* **57**, 2180 (1986).
- [11] D. Mukamel and M. B. Walker, *Phys. Rev. Lett.* **58**, 2559 (1987); O. Biham, D. Mukamel, J. Toner, and X. Zhu, *ibid.* **59**, 2439 (1987).
- [12] S. A. Langer and J. P. Sethna, *Phys. Rev. A* **34**, 5035 (1986).
- [13] G. A. Hinshaw, Jr., R. G. Petschek, and R. A. Pelcovits, *Phys. Rev. Lett.* **60**, 1864 (1988).
- [14] G. A. Hinshaw, Jr. and R. G. Petschek, *Phys. Rev. A* **39**, 5914 (1989); *Phys. Rev. B* **37**, 2133 (1988).
- [15] A. E. Jacobs and D. Mukamel, *J. Stat. Phys.* **58**, 503 (1990). The values of the wave number q given in Fig. 3 there apply to the choice $\alpha = -2$, and should be divided by $\sqrt{2}$ to correspond to Eqs. (4) there. The modulated structure proposed in Eqs. (5) (this structure corresponds to the $\Delta\phi \rightarrow 0$ case of Ref. [14]) does not give the minimum free energy.
- [16] For large $|\beta|$ ($|\beta| > 4\sqrt{\gamma a}$ at $\Delta = 0$, as discussed in Ref. [15]), the uniaxial state is unstable and a sixth-order term such as δP^6 must be added. The corresponding stability of the hexagonal state has not been investigated.
- [17] X. Qiu, J. Ruiz-Garcia, K. J. Stine, C. M. Knobler, and J. V. Selinger, *Phys. Rev. Lett.* **67**, 703 (1991).
- [18] H. Möhwald, R. M. Kenn, D. Degenhardt, K. Kjaer, and J. Als-Nielsen, *Physica A* **168**, 127 (1990).
- [19] A. M. Somoza and R. C. Desai, *J. Phys. Chem.* **96**, 1401 (1992).
- [20] J. Toner and D. R. Nelson, *Phys. Rev. B* **23**, 316 (1981).
- [21] The hexagonal solutions were obtained as follows. Fourth-order (five-point) finite-difference approximations were used for the derivatives. A rectangular grid of dimensions $(2\pi/q, \sqrt{3}\pi/q)$ consisting of 97×97 or 193×193 points was used; nodes were forced at the points of a triangular lattice of side $2\pi/q$, and symmetry conditions applied. The energy (for fixed wave number q) was minimized with respect to the function values $\sigma_x(x_i, y_i)$ and $\sigma_y(x_i, y_i)$. Results were checked using a two-dimensional Fourier expansion.